LEVEL IV

AD-E 410 174

TECHNICAL REPORT ARCSL-TR-79050

THE NATURE OF GUN SMOKE AND DUST OBSCURATION DUE TO CANNON FIRING

by

Edward W. Stuebing
Emmanuel A. Lucia
Frank D. Verderame
James J. Pinto
Robert W. Doherty
SP4 George Vinansky

Research Division

A074352

DDC FILE COPY

DDC
RECEIVED
SEP 27 1979
E

July 1979

35 p.

LT 1611 02 A 71A

US ARMY ARMAMENT RESEARCH AND DEVELOPMENT COMMAND
Chemical Systems Laboratory
Aberdeen Proving Ground, Maryland 21010

Approved for public release; distribution unlimited.

Disclaimer

The findings in this report are not to be construed as an official Department of the Army position unless so designated by other authorized documents.

Disposition

Destroy this report when it is no longer needed. Do not return it to the originator.

UNCLASSIFIED

SECURITY CLASSIFICATION OF THIS PAGE (When Data Entered)

REPORT DOCUMENTATION PAGE		READ INSTRUCTIONS BEFORE COMPLETING FORM
1. REPORT NUMBER ARCSL-TR-79050	2. GOVT ACCESSION NO.	3. RECIPIENT'S CATALOG NUMBER
4. TITLE (and Subtitle) THE NATURE OF GUN SMOKE AND DUST OBSCURATION DUE TO CANNON FIRING		5. TYPE OF REPORT & PERIOD COVERED Technical Report August 1977 6. PERFORMING ORG. REPORT NUMBER
7. AUTHOR(s) E. W. Stuebing, J. J. Pinto E. A. Lucia, R. W. Doherty F. D. Verderame, SP4 G. Vinansky		8. CONTRACT OR GRANT NUMBER(s)
9. PERFORMING ORGANIZATION NAME AND ADDRESS Commander/Director, Chemical Systems Laboratory Attn: DRDAR-CLB-PS Aberdeen Proving Ground, Maryland 21010		10. PROGRAM ELEMENT, PROJECT, TASK AREA & WORK UNIT NUMBERS 1T161102A71A Scientific Area 5
11. CONTROLLING OFFICE NAME AND ADDRESS Commander/Director, Chemical Systems Laboratory Attn: DRDAR-CLJ-R Aberdeen Proving Ground, Maryland 21010		12. REPORT DATE July 1979 13. NUMBER OF PAGES 37
14. MONITORING AGENCY NAME & ADDRESS(if different from Controlling Office)		15. SECURITY CLASS. (of this report) UNCLASSIFIED 15a. DECLASSIFICATION/DOWNGRADING SCHEDULE NA

16. DISTRIBUTION STATEMENT (of this Report)

Approved for public release; distribution unlimited.

17. DISTRIBUTION STATEMENT (of the abstract entered in Block 20, if different from Report)

18. SUPPLEMENTARY NOTES

Publication of this report was sponsored by the Army Smoke Research Program, Chemical Systems Laboratory, Aberdeen Proving Ground, Maryland. The study was conducted at Pitman-Dunn Laboratory, Frankford Arsenal under sponsorship of the Fire Control Program, but was unpublished due to closure of that laboratory.

19. KEY WORDS (Continue on reverse side if necessary and identify by block number)

Gunsmoke, Dust, Aerosols
Obscuration, Fire control, Visible
Near IR infrared

20. ABSTRACT (Continue on reverse side if necessary and identify by block number)

Fire control systems must contend with maintaining target visibility during firing. In addition, sophisticated future fire control systems have been proposed which provide an optical guidance link to the projectile, or track a fired projectile along its trajectory and sense the miss distance at the target for automatic correction. To be successful, these systems must be able to optically track the projectile during the first few seconds after firing, during which time the transparency of the atmosphere near the muzzle is very seriously degraded by ~~gun gases~~, gun smoke, and dust

(continued on reverse side)

DD FORM 1 JAN 73 1473 EDITION OF 1 NOV 65 IS OBSOLETE

UNCLASSIFIED

SECURITY CLASSIFICATION OF THIS PAGE (When Data Entered)

20. ABSTRACT (Continued)

clouds created from the ground by muzzle blast. This paper presents an analysis of optical transmission data in three wavelength regions (visible, near IR, and far IR) collected for single shot firing of a Rarden 30 mm cannon. Spectroscopic and light scattering techniques are used to identify muzzle gas and aerosol components, and a quantitative model is constructed using Mie scattering calculations to identify equivalent monodisperse aerosols for the smoke and dust. Concentrations of ammonia gas from the muzzle emission which produce significant extinction in the 10.6μm spectral region are identified and their dissipation with time is followed. Aerosol obscuration effects are found to be due to two separate aerosols arising in different time regimes after firing. Obscuration is initially attributed to a water-based gun smoke aerosol of 1.0-1.5μm particles followed in 3 to 6 seconds by a clay-based dust aerosol of 4-5μm particles rising from the ground. The evolution of each aerosol in terms of changing particle sizes and number densities is followed, and the interplay of absorption effects and scattering effects at various wavelengths is discussed.

PREFACE

This study was conducted at Pitman-Dunn Laboratory, Frankford Arsenal, Philadelphia, Pennsylvania, under the sponsorship of the Fire Control Program. It covers work which was performed through August 1977 under Project 1T161102A71A.

The use of trade names in this report does not constitute an official endorsement or approval of the use of such commercial hardware or software. This report may not be cited for purposes of advertisement.

Reproduction of this document in whole or in part is prohibited except with permission of the Commander/Director, Chemical Systems Laboratory, Attn: DRDAR-CLJ-R, Aberdeen Proving Ground, Maryland 21010; however, DDC and the National Technical Information Service are authorized to reproduce the document for United States Government purposes.

Accession For
NTIS GRA&I ☑
DDC TAB ☐
Unannounced ☐
Justification
By
Distribution/
Availability Codes
Dist | Avail and/or special
A

TABLE OF CONTENTS

	Page
INTRODUCTION	7
DATA RESOURCES	7
MODEL CONCEPT	10
APPROACH	12
SMOKE MODEL	13
DUST MODEL	21
SUMMARY	30
REFERENCES	33
DISTRIBUTION	35

LIST OF ILLUSTRATIONS

Figure		
1	Transmission vs. Time for Shot 3	8
2	Infrared Spectrum of Gun Smoke and Gases	9
3	Optical Density due to Ammonia as a Function of Time (Shot 4)	11
4	Water Number Density vs. Time	19
5	Optical Density due to Gun Smoke Model	20
6	Visible and Infrared Spectrum of Dust Sample	22
7	Infrared Spectrum of Clay	23
8	Optical Density due to Gun Smoke and Dust Model	29

PRECEDING PAGE NOT FILMED
BLANK

LIST OF TABLES

Table		Page
I.	Products of Nitrocellulose Combustion.....	15
II.	H_2O Calculation.....	16
III.	Water Aerosol Model.....	17
IV.	Model Refractive Indices for Dust.....	24
V.	Dust in Air Calculation.....	25
VI.	Clay Aerosol Model.....	26
VII.	Particle Size Composition for Aerosols Produced from Aberdeen Proving Ground Clay Samples.....	28

THE NATURE OF GUN SMOKE AND DUST OBSCURATION DUE TO CANNON FIRING

INTRODUCTION

Sophisticated future fire control systems have been proposed which track a fired projectile along its trajectory and sense the miss distance at the target for automatic correction. To be successful, the system must be able to optically track the projectile during the first few seconds after firing, during which time the transparency of the atmosphere near the muzzle is very seriously degraded by gun gases, gun smoke, and dust clouds created from the ground by muzzle blast. We here present an analysis of optical transmission data in three wavelength regions (visible, near IR, and far IR) collected for single shot firing of a Rarden 30 mm cannon, which results in a quantitative model for the gun smoke aerosol and for the dust aerosol responsible for the obscuration. The purpose of this study is to contribute data on obscuration effects which is required as part of an assessment of the relative potential of lasers operating at wavelengths of 0.53μm, 1.06μm, and 10.6μm for providing an active projectile tracking system. This study was sponsored by the Photoelectric Laboratory and by the Automatic Cannon Technology Fire Control Office of the Fire Control Development and Engineering Directorate, Frankford Arsenal.

DATA RESOURCES

The optical transmission data on which this study is based were taken from a series of experiments conducted by Heater, Pontelandolfo, and McKeough[1] at Aberdeen Proving Ground during the summer of 1974. Each shot of the Rarden 30 mm cannon was filmed and optical transmission data were recorded for a path 93 feet long, parallel to the gun-target axis and passing alongside the muzzle. These radiometric measurements were made in two optical bands of 200 Å width centered about wavelengths of 0.53μm and 1.06μm, and in a third optical band of 0.22μm width centered about 10.6μm. The films of each shot were reviewed to select for analysis one with wind conditions as quiet as possible in order to avoid confounding intrinsic aerosol effects with transmission changes due to wind moving the aerosol cloud around in the optical path; in this way shot #3 was selected for detailed analysis. The data are shown in Figure 1.

The infrared transmission spectrum over a similar optical path was available for one of the other shots (#4). The data, as reduced from the Fourier transform spectrometer recording, are shown in Figure 2.

---

[1] J. McKeough and J. Heater, "Obscuration Measurements on 30 mm Rarden Gun", FA-TR-76037, Frankford Arsenal, Philadelphia, PA 19137 (July 1976).

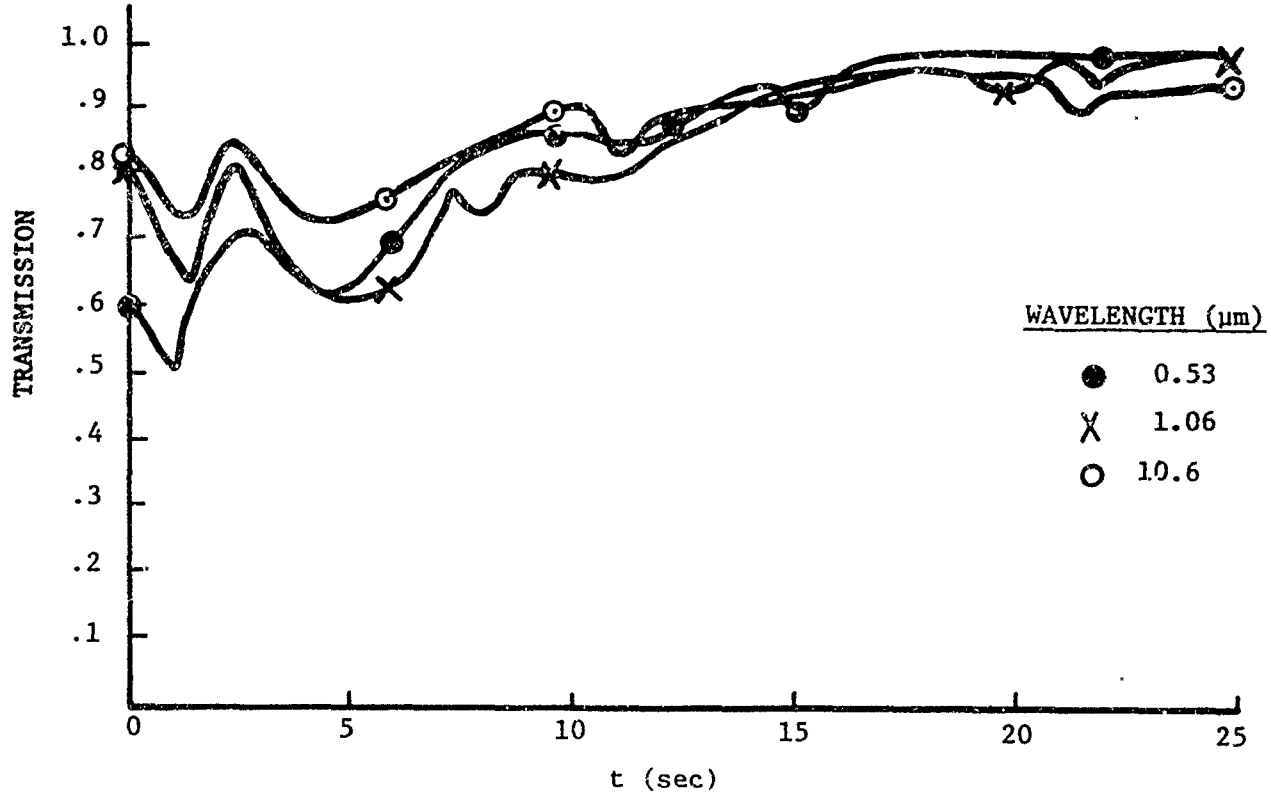

Figure 1. Transmission vs. Time (secs.) for Shot 3.

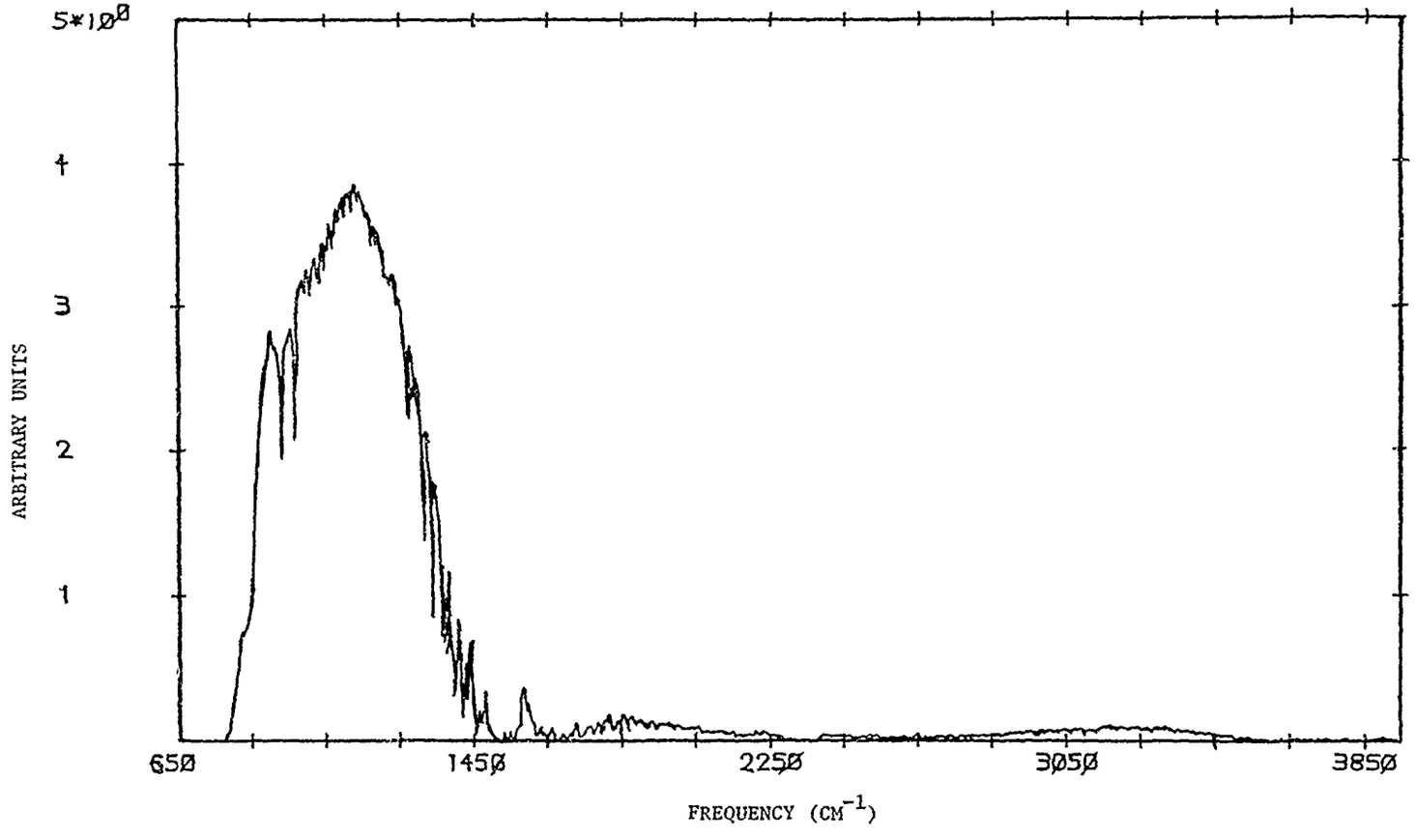

Figure 2. Infrared Spectrum of Gun Smoke and Gases.

The basic envelope of the peak in the 800-1450 cm^{-1} region is the emission of the glowing coil source. The jagged absorption bands along the high wave number side of the envelope are due to water, the strong absorption doublet in the 900-100 cm^{-1} region and nearby weaker bands are due to ammonia (NH_3). Following the decay of this doublet in time showed the time dependence of the NH_3 absorption which is plotted in Figure 3. This NH_3 absorption falls within the band pass of the 10.6μm radiometer, so that the presence of NH_3 in the muzzle gases will confound the optical data we would like to attribute to the aerosol. Because the spectrometer data were not available for shot #3, they cannot be related directly to the radiometer data of Figure 1; however, NH_3 absorption can be expected to interfere seriously with the validity of any inference on the aerosol based on 10.6μm radiometer data, especially during the first 2-3 seconds following the shot.

Samples of loose dirt were collected from the surface of the ground at three different locations near and forward of the muzzle by the experimental crew. These were made available to the authors for laboratory study.

MODEL CONCEPT

The obscuration effect will be modeled as due to two aerosols: (1) gun smoke and (2) dust created from the ground by muzzle blast. In Figure 1, the general features at all three wavelengths show a transmission minimum at about 1 1/2 seconds, rising to a maximum at 2 1/2 seconds, followed by a second minimum at 4 seconds, and then gradually rising to well above 90% as the obscuration clears. Examination of the data for all shots[1] reveals that this double minimum (min-max-min) structure within 5 seconds, followed by relatively smooth restoration of visibility, is a common feature. Viewing the films of the shots shows that first a greyish-white smoke cloud forms in the air in front of the muzzle almost instantly on firing (it does not appear to issue from the muzzle as smoke, rather the smoke forms in the air), and second, the muzzle blast shock wave can be seen racing along the ground sweeping along a low-lying dust skirt which then rises in a swirling, turbulent cloud after the shock wave has passed. By timing the visible effect on the screen, this dust cloud appears to reach the optical path of the radiometers (about shoulder high) in 3 to 5 seconds after firing. This agrees in time with the appearance of the second transmission minimum.

[1] J. McKeough and J. Heater, "Obscuration Measurements on 30 mm Rarden Gun", FA-TR-76037, Frankford Arsenal, Philadelphia, PA 19137 (July 1976).

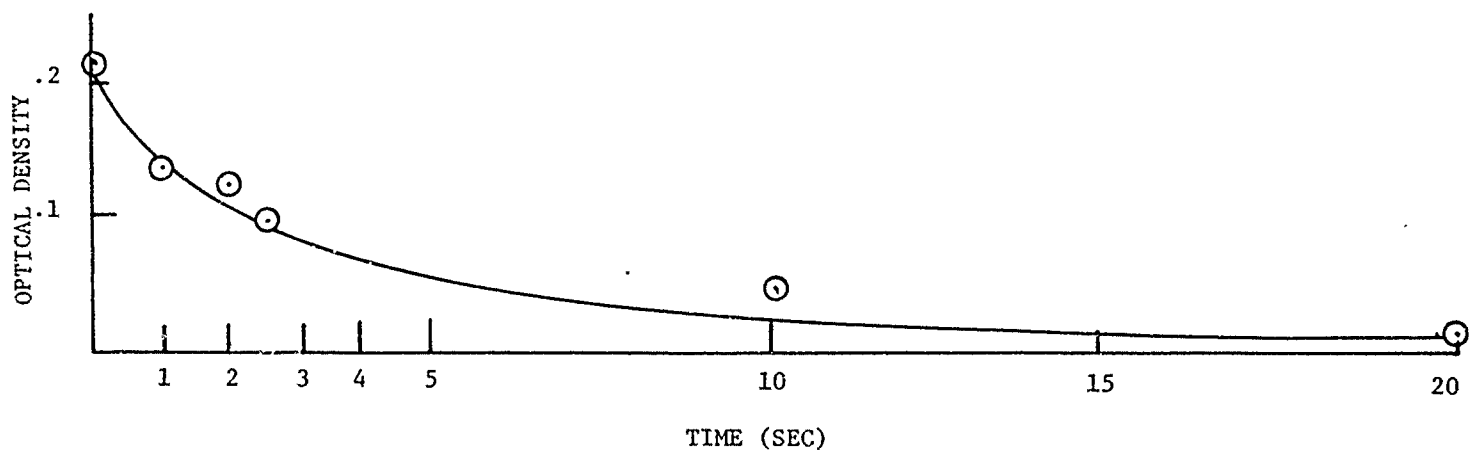

Figure 3. Optical Density Due to Ammonia as a Function of Time (Shot 4), $\nu = 930\ cm^{-1}$.

We propose then the following concept model. The initial obscuration is due to gun smoke which for reasons identified below increases in opacity for the first second or so and then dissipates. As the smoke cloud dissipates, the dust cloud rising from the ground enters the optical path resulting in increasing opacity for a while and then dissipates. The min-max-min transmission behavior is then attributed to smoke-dissipation-dust-dissipation. The following sections explore the detailed nature of these two aerosols based on the data for Shot #3 (Figure 1).

APPROACH

In an extinguishing medium a light beam is attenuated according to

$$I = I_o e^{-\varepsilon C \ell} \tag{1}$$

where I is the transmitted intensity, I_o is the incident intensity, ε is an extinction coefficient, and C and ℓ are the concentration and path length in the medium in units appropriate to those used to specify ε. In aerosol studies C is commonly given as a number density in units of particles per cm^3 and ℓ is given in meters. The extinction coefficient ε is then in units of cm^3/m which is an area (i.e., 10^{-2} cm^2), and has a particular value for any given particle depending on its composition (refractive index) size, shape, and the wavelength of light incident on it. Assuming spherical particles, then from the wavelength, particle size, and refractive index the extinction cross-section (C_{ext}) may be calculated using the well known Mie theory.[2] In general the particle may be composed of a material which absorbs light at the wavelength of interest so that the observed extinction will be due to absorption as well as scattering. In this case the refractive index will be a complex number with an imaginary component related to the degree of absorption. Therefore, performing such calculations with accuracy will require knowing the real and imaginary components of the refractive index, at the wavelengths of interest, for the material of which the aerosol particles are composed.

The transmission (T) as reported in Figure 1 is the ratio of transmitted to incident light intensity. Then from Equation (1)

---

[2] E. W. Stuebing, J. J. Pinto (FA), and R. B. Gomez (Atmos. Sci. Lab), "PGAUSS-LT: A Program for Computing Optical Properties of Single Scattering Aerosol Clouds of Homogeneous Particles", FA-TM-75019, Frankford Arsenal, Philadelphia, PA 19137 (April 1975).

$$T = I/I_o = e^{-\varepsilon C \ell} \tag{2}$$

The transmission is not conveniently related to the parameters ε and C which are directly related to the aerosols we wish to characterize. Therefore, the transmission data is digitized at 0.5 second intervals and converted to optical densities (OD)

$$OD = -\log T = (1/2.303)\varepsilon C \ell \tag{3}$$

which provide a more convenient linear relationship. The experiment is then analyzed by seeking model aerosols for which values of ε, C, and ℓ can be derived which will lead to OD vs. time curves in agreement with the data.

The approach may be summarized as follows. First, a candidate material for the aerosol particles is chosen and real and imaginary components for its refractive index are selected at each of the three wavelengths for which experimental data were collected. Second, a series of Mie scattering calculations are performed at each wavelength for spherical particles of this material at a variety of particle diameters. Third, an effective particle diameter in the cloud must be selected at each point in time. This is done by comparing the observed ratios of extinction at the various wavelengths [OD(0.53μm)/OD(1.06μm) and OD (0.53μm)/OD(10.6μm)] to the ratios predicted from the Mie calculation for the various sized particles. Because the amount of extinction depends strongly on the ratio of particle size to wavelength, this measure can be used as a sensitive indicator of particle size. Unfortunately, it is not always unique to a single particle size, as we shall see. Finally, with ε fixed by the choice of refractive index and the choice of particle size selected from the ratios of OD's at different wavelengths, the product $C\ell$ can be determined to agree with the magnitude of the observed extinction. For convenience in reporting we shall take the cloud to be unitform over the 93 foot path length and report C as an effective number density (units = cm^{-3}).

SMOKE MODEL

The early obscuration phenomena including the first transmission minimum to the maximum at 2.5 seconds is to be attributed to gun smoke. As pointed out previously, the presence of significant amounts of NH_3 in the vicinity of the muzzle is to be expected during this time and confound the extinction data in the 10.6μm region. We shall, therefore, rely on the data at 0.53μm and 1.06μm in constructing the gun smoke model.

The presence of significant amounts of NH_3 is to be expected following the combustion of nitrocellulose base propellants. The products of nitrocellulose combustion are shown in Table I. The water gas reaction follows an equilibrium appropriate to the high temperature, high pressure conditions inside the bore as the projectile travels down the barrel. When the projectile exits from the muzzle there is a sudden, catastrophic loss of temperature and pressure which freezes the concentrations at essentially those typical of the in-bore high temperature, high-pressure environment. Under these conditions there is an equilibrium established between the H_2 in the water gas reaction, the N_2, and NH_3 which results in the observed significant concentrations of NH_3. Note that gaseous water will also be released and suddenly cooled as the projectile exits the muzzle. Also a variety of hygroscopic metals and metal oxides are present from propellant additives or primer mixes. These can be expected to form active condensation nuclei for the suddenly cooled water resulting from propellant combustion, and for atmospheric water in the vicinity of the muzzle. Water droplets are, therefore, selected as a model material for the gun smoke aerosol. This water is certainly contaminated with a variety of materials, however, without further data on chemical composition, it seems a reasonable first approximation to model the gun smoke as a pure water aerosol.

The results of Mie calculations on water drops are given in Table II. The complex indices of refraction at the wavelengths of interest are shown in the box. From the magnitude of the imaginary components it is clear that pure water has effectively no absorption at 0.53 and 1.06μm, and moderate absorption at 10.6μm. For various particle diameters, the optical density per particle/cm^3 per meter path length [cf., ε in Equation (3)] is given for each wavelength along with the ratio of these extinctions at the two wavelengths of principal interest.

The development of the water aerosol model is shown in Table III. At each of the 0.5 second intervals, the observed ratio of extinction at the two wavelengths is shown. Referring to the theoretical results in Table II allows the identification of an effective particle diameter. Of course the actual aerosol will be polydisperse (i.e., have a distribution of particle sizes); we model it here in terms of an equivalent monodisperse aerosol. For example, at time zero the measurements show an OD at the 0.53μm wavelength 2.4 times greater than the OD at 1.06μm. Referring to Table II shows that for drops of pure water this ratio would be expected from drops 1.0μm in diameter. Then considering the absolute OD's actually observed at 0.53μm and 1.06μm and the cross sections ε of a 1.0μm water drop at these two wavelengths, one finds from Equation (3) the required number density in the two cases to be 5.3×10^3 and 5.8×10^3, which are assigned as the range of uncertainty, and for the model a value of 5.6×10^3 is chosen. This process is repeated at each half second interval up to 2.5 seconds.

TABLE I. PRODUCTS OF NITROCELLULOSE COMBUSTION

Major Products

CO, CO_2, H_2, H_2O (Water Gas Equilibrium)

N_2

Major Minor Products

CH_4, NH_3

Minor Minor Products

C, K_2O, SnO_2, Na_2O, BaO

(Pb, Sb, Si, Zr, Ca, Al)

Wavelength	Refractive Index
0.53	1.335 (1-0.000000001)
1.06	1.325 (1-0.000000808)
10.6	1.182 (1-0.06091)

TABLE II. H_2O CALCULATION

DIAM. (μm)	OD/PART/METER 0.53	1.06	10.6	OD 0.53 / OD 1.06
0.1	0.464(-10)	0.282(-11)	0.179(-10)	16.5
0.5	0.150(-6)	0.258(-7)	0.225(-8)	5.81
0.9	0.104(-5)	0.367(-6)	0.133(-7)	2.83
1.0	0.134(-5)	0.565(-6)	0.183(-7)	2.37
1.1	0.164(-5)	0.824(-6)	0.245(-7)	1.99
1.2	0.182(-5)	0.112(-5)	0.320(-7)	1.62
1.3	0.195(-5)	0.150(-5)	0.409(-7)	1.30
1.4	0.210(-5)	0.193(-5)	0.517(-7)	1.09
1.5	0.210(-5)	0.238(-5)	0.637(-7)	0.88
1.6	0.195(-5)	0.295(-5)	0.778(-7)	0.66
1.7	0.201(-5)	0.351(-5)	0.941(-7)	0.57
1.8	0.215(-5)	0.405(-5)	0.113(-6)	0.53
1.9	0.207(-5)	0.475(-5)	0.134(-6)	0.44
2.0	0.233(-5)	0.530(-5)	0.157(-6)	0.44
5.0	0.176(-4)	0.220(-4)	0.326(-5)	0.80
10.0	0.687(-4)	0.692(-4)	0.332(-4)	0.98
20.0	0.292(-3)	0.278(-3)	0.278(-3)	1.05

TABLE III. WATER AEROSOL MODEL

TIME	OBSERVED $\frac{OD(0.53)}{OD(1.06)}$	DIAM. (μm)	N_{H_2O} (UNITS = 10^3) RANGE	MODEL
0.0	2.4	1.0	5.3 - 5.8	5.6
0.5	2.1	1.1	5.3 - 5.4	5.4
1.0	1.7	1.2	5.4 - 5.6	5.5
1.5	1.1	1.4	3.4 - 3.6	3.5
2.0	1.2	1.35	2.8 - 2.9	2.8
2.5	1.1	1.4	1.4 - 2.3	1.8
3.0		1.4		1.2
3.5		1.4		.85
4.0		1.4		.60
4.5		1.4		.42
5.0		1.4		.29
6.0		1.4		.20
7.0		1.4		.07
8.0		1.4		.034
9.0		1.4		.017
10.0		1.4		.008
15.0		1.4		.002

Note that during the first 1 1/2 seconds the particle number density remains rather constant while the drops grow in size from 1.0 to 1.4μm. After this the drop size remains stable while the cloud dissipates.

After 2.5 seconds the effect of the rising dust aerosol dominates the observed extinction. Nevertheless, there remains a significant amount of water whose effect must be subtracted from the observed OD data in order to characterize the dust aerosol. A plot of H_2O drop number density vs. time, Figure 4, shows that once droplet growth stops and the water cloud begins to dissipate, the reduction in log (N) appears to be quite linear as shown by the circled points. This trend was simply extrapolated, number density values read at successive 1/2 second intervals [triangles in Figure 4], and the droplets assumed to remain stabilized at 1.4μm diameter. The results are shown below the dotted line in Table III. Table II data then allows the calculation of remaining OD due to dissipating water at each wavelength.

The OD effects due to the final water model are shown in Figure 5, where the circled points show the experimental data, and crosses plot the effect contributed by the water model of Table III. The behavior at 0.53μm and 1.06μm is very well reproduced, with the exception of the point at 2.5 seconds. This is the cross-over point at the transition between a smoke-dominated cloud and a dust-dominated cloud; it would be reasonable to expect significant contributions from both aerosols here. As the model attempts to account for the effect entirely in terms of the smoke aerosol, it is not surprising that the agreement is less than perfect. Note also that this model cannot explain the observed obscuration at 10.6μm at all. In the context of our model concept this must be left to the effects of NH_3 gas absorption or contaminants which certainly must be present in the water. It seems unlikely that these water impurities would absorb significantly at the 0.53 and 1.06μm wavelengths because the cloud has no apparent color, therefore, the refractive index of the particles at these two wavelengths is not expected to differ greatly from that of pure water. Furthermore, the 1.0-1.4μm diameter particles are on the order of the same size as these two wavelengths, a condition which causes the extinction to be strongly dominated by scattering rather than absorption. On the other hand, 10.6μm radiation has a wavelength much longer than the particle size. This leads to considerably enhanced absorption in the overall extinction. If absorbing impurities are present in the water, they would be expected to most strongly affect the 10.6μm wavelength.

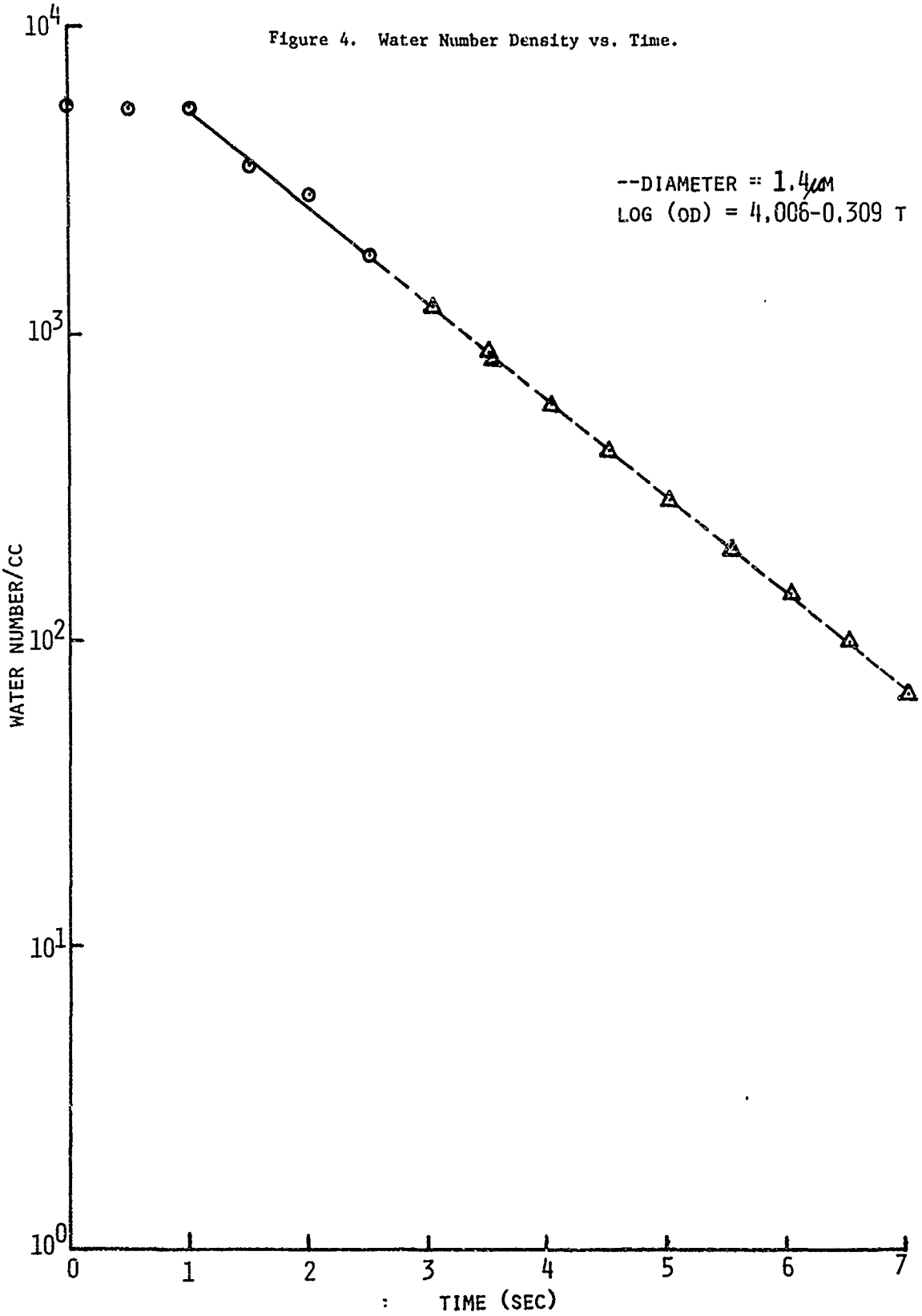

Figure 4. Water Number Density vs. Time.

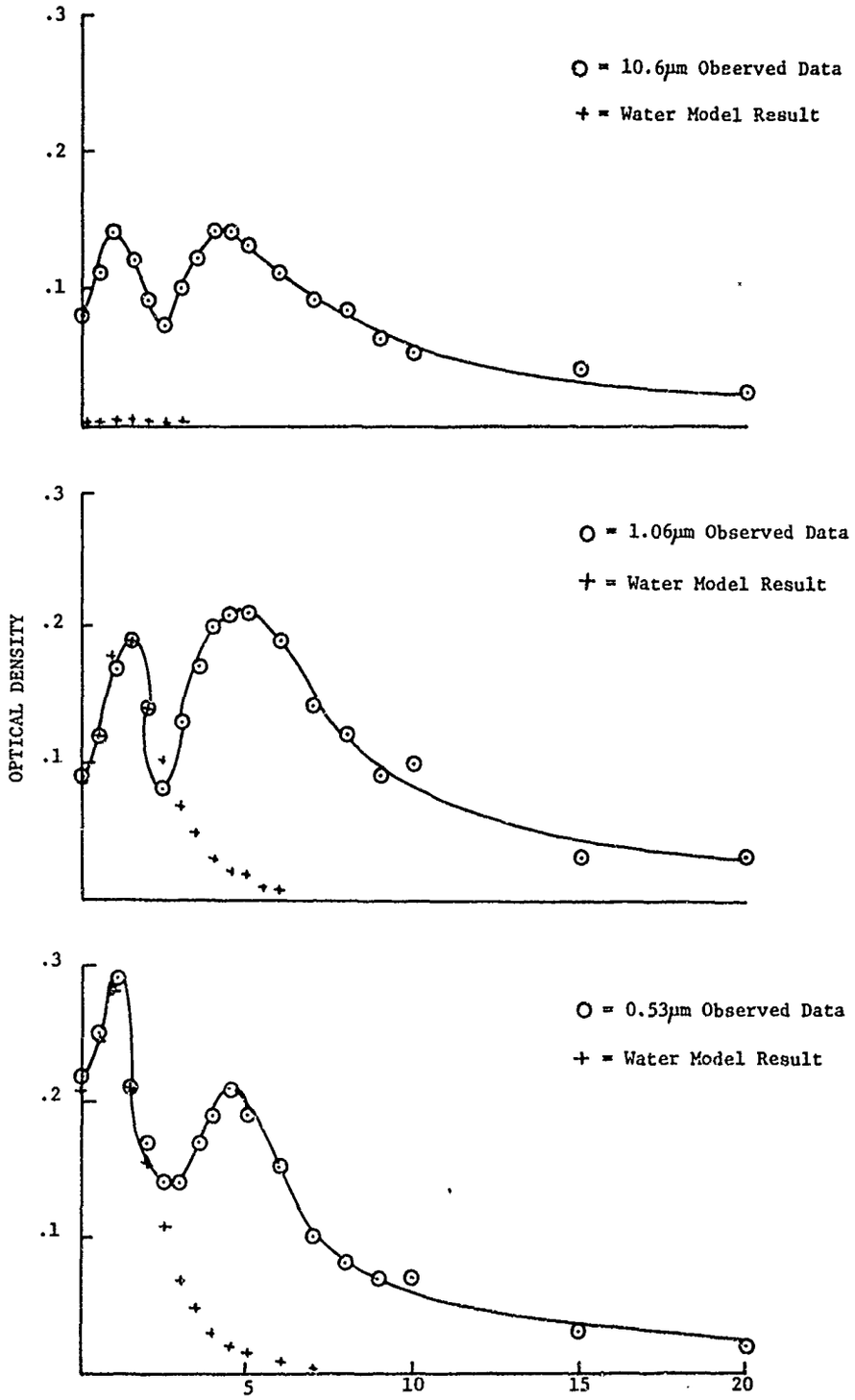

Figure 5. Optical Density Due to Gun Smoke Model.

DUST MODEL

In order to establish a model refractive index for the dust particles comprising the aerosol, the dirt samples returned from the experiment site were examined. After sieving, the fines passing through a #320 mesh screen were mulled with KBr and pressed to form a pellet for spectroscopic study. The spectrum in the visible and infrared is shown in Figure 6. The KBr host is transparent in the visible; its IR spectrum is shown with that of the dust in order to sort out which features are to be attributed to the dust sample. In the visible, the smooth featureless increase in transmission with wavelength indicates: (1) only scattering processes are attenuating light in the sample, and (2) the particles responsible are not small compared to the wavelength because the increase is not sufficiently rapid (for very small particles compared to wavelength, Rayleigh scattering conditions obtain and the extinction follows λ^{-4}). The infrared spectrum shows a variety of absorption features. The infrared spectrum of a clay of known composition is shown in Figure 7 with the absorption features identified in terms of their origin on various components of the clay.[3] By comparison of the absorption features of Figures 6 and 7, it is clear that the dust sample is a clay.

From the literature, refractive index values typical of rural aerosols were taken for 0.53 and 1.06μm.[4] However, absorptions are expected to strongly influence extinction at the long 10.6μm wavelength, and clays of various compositions show absorptions at 10.6μm which vary over a wide range (greater than an order of magnitude). Therefore, in addition to a typical refractive index at 10.6μm[5], calculations were conducted for imaginary refractive index components at the lower and upper bounds expected for commonly occurring clays.[3] All of the refractive indices are given in Table IV.

---

[3] G. Hoidale, Atmospheric Sciences Laboratory, US Army Electronics Command, White Sands Missile Range, New Mexico, Private Communication.

[4] G. Hansel, "Computation of the Extinction of Visible Radiation by Atmospheric Aerosol Particles as a Function of the Relative Humidity, Based upon Measured Properties", Aerosol Sci. (1972).

[5] K. Fischer, "Bestimmung der Absorption von sichtbarer Strahlung durch Aerosolpartlikeln", Beitr. Phys. Atm. 43, p. 244 (1971).

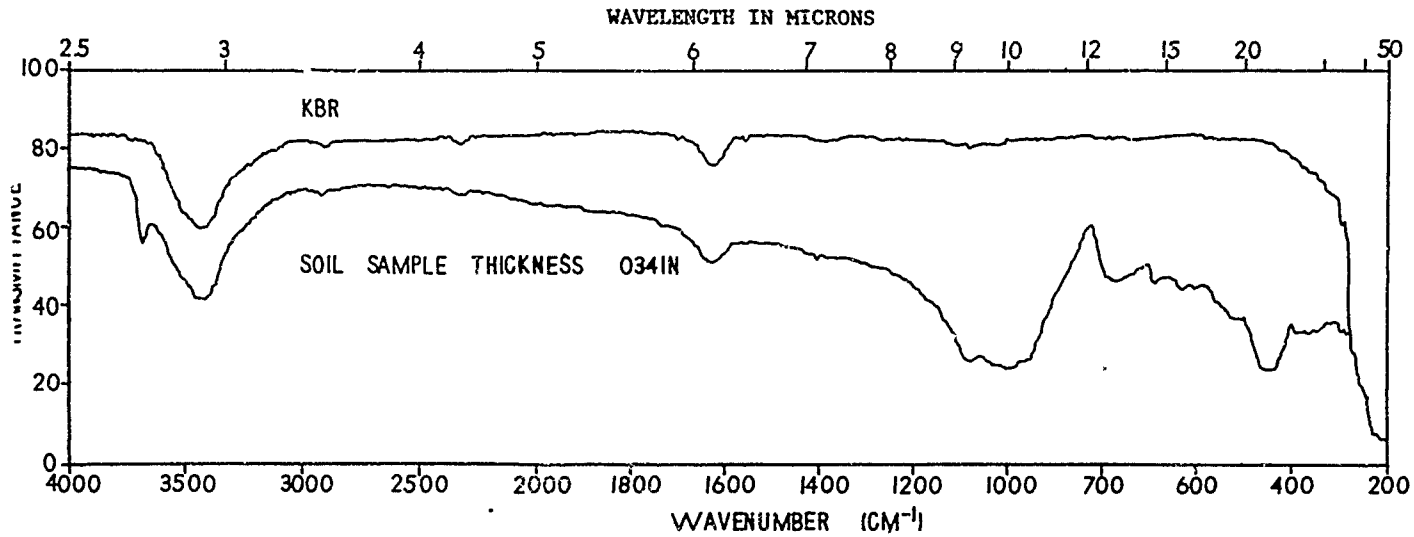

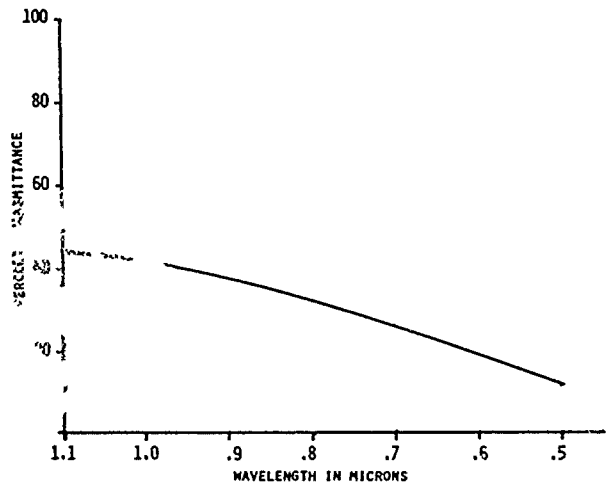

Figure 6. Visible and Infrared Spectrum of Dust Sample.

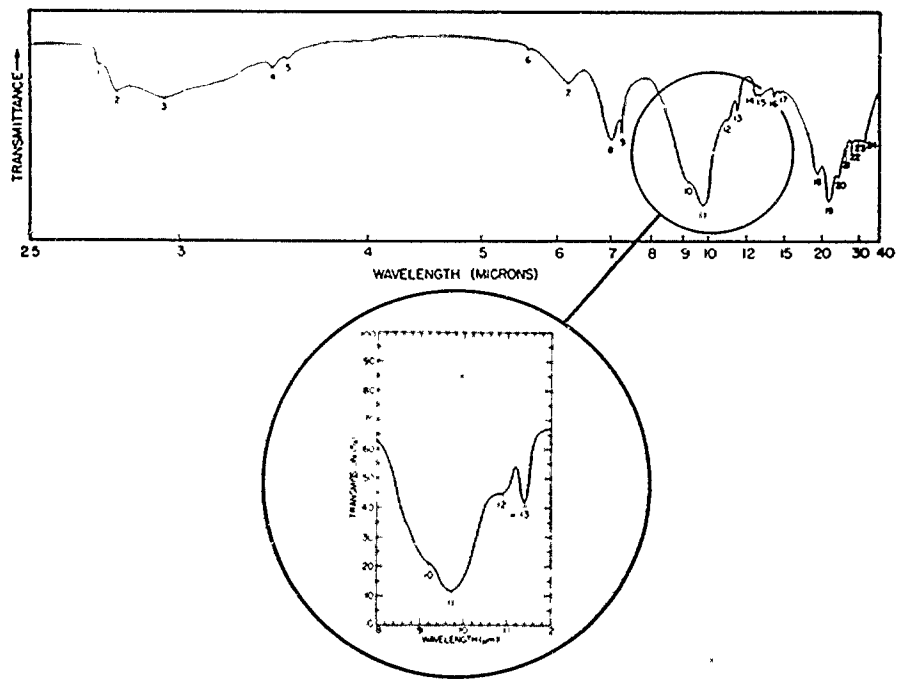

BAND	λ(μm)	COMPONENT (S)
1	2.7	KAOLIN GROUP
2	2.8	KAOLIN GROUP
3	2.9	WATER (ABSORBED,ADSORBED)
4	3.4	HYDROCARBON
5	3.5	HYDROCARBON
6	5.6	CALCITE
7	6.2	WATER (ABSORBED, ADSORBED)
8	7.0	CARBONATE (MAINLY CALCITE)
9	7.2	NITRATE
10	9.2	QUARTZ, ILLITE, MONTMORILLONITE
11	9.7	ILLITE, MONTMORILLONITE, KAOLINITE
12	10.9	ILLITE, MONTMORILLONITE, KAOLINITE

BAND	λ(μm)	COMPOSITION (S)
13	11.4	CALCITE
14	12.5	QUARTZ, KAOLINITE
15	12.9	QUARTZ
16	14.0	CALCITE
17	14.4	QUARTZ, KAOLINITE
18	19.2	QUARTZ, ILLITE, MONTMORILLONITE, KAOLINITE
19	21.4	QUARTZ, ILLITE, MONTMORILLONITE, KAOLINITE
20	23.1	ILLITE, KAOLINITE
21	25.3	QUARTZ, KAOLINITE
22	26.9	QUARTZ, KAOLINITE
23	29.2	KAOLINITE
24	31.7	CALCITE

COMPONENT	~% BY WEIGHT
MONTMORILLONITE	35
KAOLINITE	20
ILLITE	20
CALCITE	15
QUARTZ	5
OTHER	5

Figure 7. Infrared Spectrum of Clay.

TABLE IV. MODEL REFRACTIVE INDICES FOR DUST

WAVELENGTH (μm)	REFRACTIVE INDEX[a]
0.53	1.51 (1.0 - 0.0093)
1.06	1.49 (1.0 - 0.01342)
10.6 (typical)	1.67 (1.0 - 0.0808)
10.6 (min)	1.67 (1.0 - 0.0599)
10.6 (max)	1.67 (1.0 - 1.1078)

[a]See text for identification of literature sources.

Mie calculations were performed at a variety of particle diameters and the ratios OD(0.53)/OD(1.06) and OD(0.53)/OD(10.6) constructed. These are tabulated in Table V. The listed values at 10.6μm are those for the typical refractive index, with the range of results for the minimum and maximum 10.6μm absorptions shown in parenthesis. The ratio OD(0.53)/OD(1.06) is an oscillating function of particle size, hence unique assignment of particle size based on this ratio alone is not possible. The ratio OD(0.53)/OD(10.6) is a monotonically decreasing function of particle size for fixed refractive index; furthermore, the range of values about the "typical" value is quite small for large particles (absorption has little effect as particles approach the wavelength in size) and grows to reflect the order of magnitude variation in imaginary refractive index component as absorption dominates extinction with particles small compared to the wavelength.

The experimental optical density data for 3.0 seconds and later were adjusted by subtracting the effect of the water model shown in Figure 5. The residual OD at each wavelength is then to be attributed to the dust aerosol. Ratios for this adjusted experimental data are shown in Table VI along with size and number density values characterizing two possible dust aerosol models to fit this data. At 3.0 seconds the ratio OD(0.53)/OD(1.06) from Table VI could be satisfied by particles of diameter 3.0μm or 5.0μm (of Table V). By 3.5 seconds, this ratio has dropped somewhat. Table V shows that this change in behavior could be accomodated at either 3 or 5μm particles and at both sizes this decrease in ratio could be accounted for by particles either growing or shrinking! Referring to the second ratio in Table VI [OD(0.53)/OD(10.6)] shows a consistent increase in this value between 3.0 and 5.0 seconds. Recalling the Table V monotonic theoretical

TABLE V. DUST IN AIR CALCULATION

DIAM. (μm)	OD (0.53) / OD (1.06)	OD (0.53) / OD (10.6)
1.1	0.69	27.3 (36.2 - 3.2)
1.5	0.59	17.6 (22.7 - 2.0)
2.0	0.87	11.0 (14.0 - 1.3)
2.5	1.03	6.1 (7.4 - 0.82)
3.0	1.08	4.4 (5.1 - 0.76)
3.5	0.80	2.7 (3.1 - 0.66)
4.0	0.89	2.1 (2.4 - 0.72)
4.5	0.96	1.5 (1.6 - 0.67)
5.0	1.07	1.25 (1.3 - 0.72)
5.5	0.91	0.96 (0.98 - 0.66)
6.0	0.92	0.90 (0.90 - 0.69)
6.5	0.94	0.80 (0.79 - 0.67)
7.0	1.04	0.77 (0.77 - 0.70)

TABLE VI. CLAY AEROSOL MODEL

TIME	DATA		MODEL 1		MODEL 2	
	OD(0.53)/OD(1.06)	OD(0.53)/OD(10.6)	DIAM. (μm)	N (cm^{-3})	DIAM. (μm)	N (cm^{-3})
0.0						
0.5						
1.0						
1.5						
2.0						
2.5						
3.0	1.09	0.76	4.8	140	2.55	500
3.5	1.02	1.00	4.6	280	2.4	1075
4.0	0.95	1.17	4.5	380	2.35	1425
4.5	0.94	1.33	4.4	450	2.35	1640
5.0	0.89	1.35	4.1	480	2.1	1770
6.0	0.75	1.20			1.8	[a] 1600
7.0	0.74	1.09			1.8	1170
8.0	0.63	1.00			1.8	1000
9.0	0.78	1.19			1.8	815

a. See text.

trend in this ratio for fixed refractive index (whatever the refractive index is for the particular Aberdeen dust, it is fixed in value), it is apparent that particle sizes are decreasing during this time.

Two possible models then explain the experimental data. One has dust particles of about 5μm diameter present at 3.0 seconds after firing with size diminishing thereafter; the second starts at particles of about 3μm and again reduces in size with time. This reduction in size with time is reasonable as the heavy particles will be the first to settle out of the dust cloud. Extensive Mie calculations to fill in data between the diameters shown in Table V lead to the assignment of particles sizes shown in Table VI. As with the water aerosol model, number densities are then calculated to provide the magnitude of obscuration observed. At 6.0 seconds and beyond, the obscuration curves at the various wavelengths come close together so that small variations (within experimental noise) cause them to cross and result in rather wild variations in the critical ratios. A reliable analysis of this data is not possible. For the 5μm model the OD(0.53)/OD(1.06) ratio cannot be matched; for the 3μm model this first ratio can be approximately satisfied by the 1.8μm diameter particles shown in Table VI, but these particles cannot match the OD(0.53)/OD(10.6) ratio even within the widest limits of reasonable 10.6μm absorption behavior (hence the dotted line flagging this data in Table VI is used to indicate unreliability). In general, the observed 10.6μm obscuration behavior falls closer to the middle of the range of expected refractive indices for the model using 5μm diameter particles than for the 3μm particle model which would require a clay composition of extremely strong absorption properties.

The three sieved dust samples returned to the laboratory were used to produce aerosols by shocking a container in which they rested and drawing the resulting dust cloud through a five-stage Battelle impactor for particle size analysis. The results for each of the three samples are shown in Table VII. The mean particle sizes agree with Model 1. As a check on the validity of the theoretical approach used in this study, each of these polydisperse aerosols from Table VII was used as the basis of a Mie calculation, the results of which were used to construct the ratios OD(0.53)/OD(1.06) for the separate polydispersions. Using each of these ratios to enter Table V, the predicted particle size for an equivalent monodisperse aerosol was found. These are shown in the last row of Table VII. The agreement with the actual mean particle sizes is remarkably good!

The final results of the clay dust model combined with the water smoke model are shown in Figure 8. At times of 3.0 seconds and greater the optical density due to water (crosses) and that due to clay (triangles) will add together to closely reproduce the experimental results at 0.53 and 1.06μm. At 10.6μm the range of results for the two

TABLE VII. PARTICLES SIZE COMPOSITION (%) FOR AEROSOLS PRODUCED FROM ABERDEEN PROVING GROUND CLAY SAMPLES

PARTICLE DIAMETER (μm)	SAMPLE LOCATION		
	MUZZLE	ROYCO	LAMP
8	15.7	20.7	9.0
4	79.1	69.0	83.4
2	4.6	8.8	5.4
1	0.5	1.3	1.4
0.5	0.1	0.2	0.8
TOTAL	100	100	100
	PARTICLE SIZE (μm)		
Mean Particle Size	4.5	4.6	4.2
Equivalent Monodisperse[a]	4.3	4.4	4.2

[a] See text

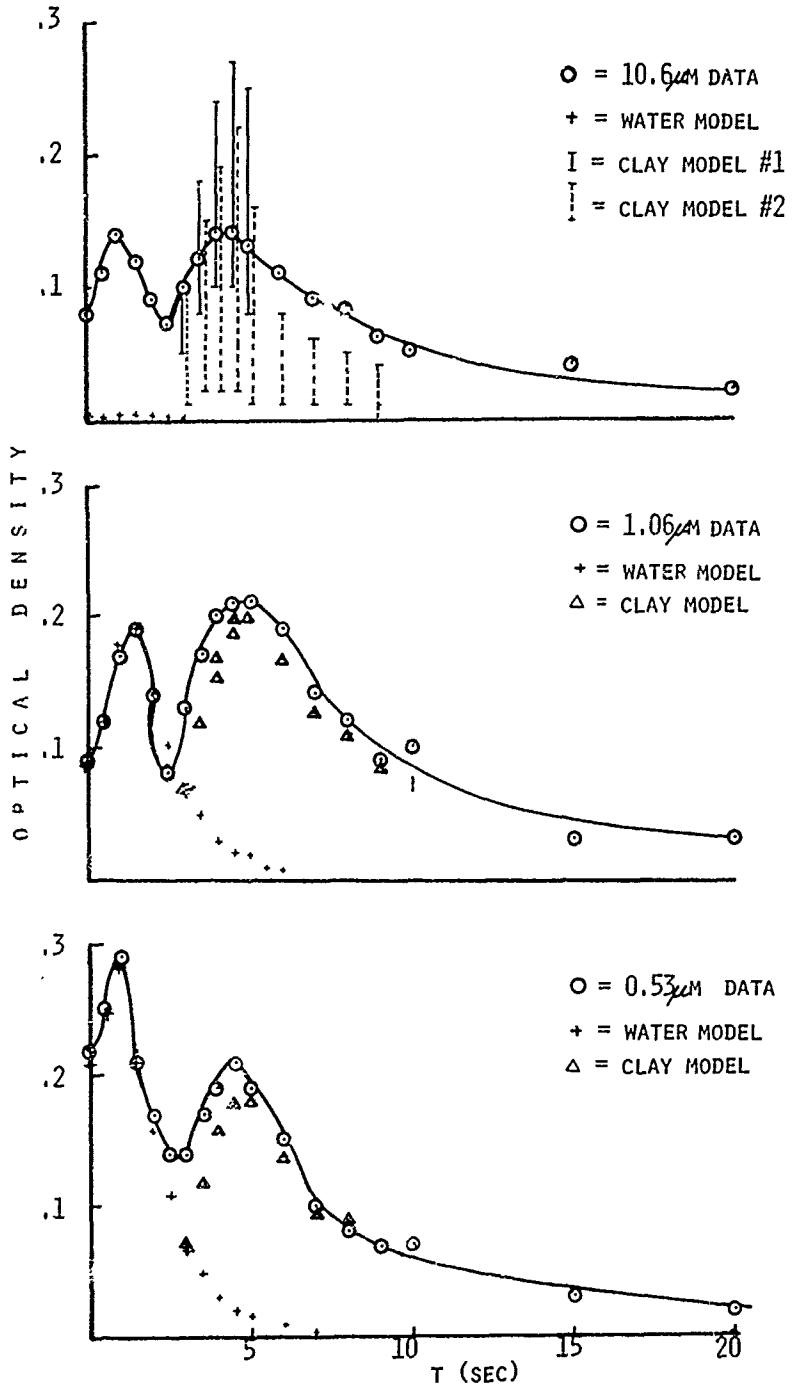

Figure 8. Optical Density Due to Gun Smoke and Dust Model.

clay models is indicated. The observed effects would be expected from a rather ordinary clay in Model 1; for Model 2 to be correct the clay would have to have been composed of an unusually strongly absorbing species. Because scattering strongly dominates the extinction at 0.53 and 1.06μm, and because the real components of the refractive indices of clays do not vary greatly, the observed extinction at these short wavelengths would be expected to be reasonably transferable to other geographical locations (types of clays). The indicated range of obscuration at 10.6μm can be read as suggesting the range of effects that might be found at other sites and hence suggests that "worst-case" conditions could result in twice the 10.6μm optical density observed during Aberdeen Proving Ground tests.

SUMMARY

The obscuration due to single shot firing of the Rarden 30 mm cannon is modeled as resulting from two different monodisperse aerosols arising sequentially in time. The first aerosol, gun smoke, is composed of water drops condensed upon expansion of the water vapor product of propellant combustion and of atmospheric water vapor precipitated on condensation nuclei formed from propellant and primer combustion. This smoke cloud forms in front of the muzzle within a small fraction of a second after the projectile exits. Initially particles are spherical drops of about 1.0μm diameter which grow during the first second of time to 1.4μm without decrease in number density. As a result obscuration increases during this first second. Thereafter, particle size remains constant and dissipation of the aerosol results in decreased number density and obscuration. By three seconds, clay dust, which has been rising from the ground following the muzzle blast wave, begins to reach the height of the muzzle in quantities which produce more obscuration than the remaining smoke cloud. Particle diameter at three seconds is probably near 5μm, although it would be possible for particles of about half this size to also satisfy the optical data. In either case particle size decreases with time thereafter due to settling of the heavier particles. The rising dust cloud causes continuously increasing number density at the muzzle level during the period from three to six seconds; however, the effect of the concommitant decrease in particle size results in increasing obscuration only up until the fifth second, after which time visibility continuously improves as the cloud settles and dissipates.

These smoke and dust aerosol models agree well with the optical data at 0.53μm and 1.06μm wavelengths. In these cases, the obscuration is due to scattering which is a process not strongly dependent on wavelength. Therefore, the data gathered using radiometers with relatively

large band pass filters should also be representative of the effect that would have been observed had lasers operating at these wavelenghts been used. The 10.6μm wavelength effects are not due to the aerosols alone; there are significant gas absorptions in this region due to ammonia produced by propellant combustion. In addition, the gun smoke aerosol based on pure water cannot account for the observed 10.6μm effect. It must, therefore, be attributed to absorptions due to contaminations which are certainly present in the water or to the ammonia gas absorption. The ammonia absorption is a doublet falling almost entirely within the band pass of the radiometer; however, the 10.6μm wavelength itself falls on the high transmission spike between the absorption doublet. Therefore, the 10.6μm radiometer results are not expected to be typical of 10.6μm laser effects, the laser being expected to be superior in transmission, particularly during the first two seconds after firing.

Finally, unlike the results at wavelengths of 0.53 and 1.06μm, the 10.6μm wavelength results, even for aerosol effects, are due principally to absorption rather than scattering. This is particularly true of the dust obscuration, in which case the optical density can be expected to vary by a factor of three depending on the geographical location (i.e., chemical composition of the clay). The obscuration at 0.53 and 1.06μm wavelengths is due to scattering and is relatively insensitive to clay species or water impurities. Therefore, the 0.53μm and 1.06μm data is more likely transferable from location to location, with some dependence in the gun smoke expected on local conditions of relative humidity.

REFERENCES

1. J. McKeough and J. Heater, "Obscuration Measurements on 30 mm Rarden Gun", FA-TR-76037, Frankford Arsenal, Philadelphia, PA 19137 (July 1976).

2. E. W. Stuebing, J. J. Pinto (FA), and R. B. Gomez (Atmos. Sci. Lab), "PGAUSS-LT: A Program for Computing Optical Properties of Single Scattering Aerosol Clouds of Homogeneous Particles" FA-TM-75019, Frankford Arsenal, Philadelphia, PA 19137 (April 1975).

3. G. Hoidale, Atmospheric Sciences Laboratory, US Army Electronics Command, White Sands Missile Range, New Mexico, Private Communication.

4. G. Hansel, "Computation of the Extinction of Visible Radiation by Atmospheric Aerosol Particles as a Function of the Relative Humidity, Based upon Measured Properties", Aerosol Sci. (1972).

5. K. Fischer, "Bestimmung der Absorption von sichtbarer Strahlung durch Aerosolpartlikeln", Beitr. Phys. Atm. 43, p. 244 (1971).

PRECEDING PAGE NOT FILMED BLANK

DISTRIBUTION LIST FOR ARCSL-TR-79050

Names	Copies
Chemical Systems Laboratory	
Aberdeen Proving Ground, MD 21010	
Office of the Director	
Attn: DRDAR-CLG	1
CB Detection & Alarms Division	
Attn: DRDAR-CLC	1
Developmental Support Division	
Attn: DRDAR-CLJ-L	3
Attn: DRDAR-CLJ-R	3
Attn: DRDAR-CLJ-M	1
Munitions Division	
Attn: DRDAR-CLN	1
Attn: DRDAR-CLN-S	1
Physical Protection Division	
Attn: DRDAR-CLW-P	1
Research Division	
Attn: DRDAR-CLB	1
Attn: DRDAR-CLB-B	1
Attn: DRDAR-CLB-P	1
Attn: DRDAR-CLB-T	1
Attn: DRDAR-CLB-PS (Mr. Vervier)	1
Attn: DRDAR-CLB-PS (Dr. Stuebing)	1
Attn: DRDAR-CLB-PS (Mr. Frickel)	1
Systems Development Division	
Attn: DRDAR-CLY-A	1
Attn: DRDAR-CLY-R	6
DEPARTMENT OF DEFENSE	
Administrator	
Defense Documentation Center	
Attn: Document Processing Division (DDC-DD)	12
Cameron Station	
Alexandria, VA 22314	
Office of the Director	
Defense Research and Engineering	
Attn: Dr. T.C. Walsh, Rm 3D-1079	1
Washington, DC 20310	
Institute for Defense Analysis	
400 Army-Navy Drive	
Attn: L. Biberman	1
Attn: R. E. Roberts	1
Arlington, VA 22202	
Advanced Research Projects Agency	1
1400 Wilson Boulevard	
Arlington, VA 22209	

Names	Copies
DEPARTMENT OF THE ARMY	
Commander	
US Army Research Office – Durham	1
Box CM, Duke Station	
Durham, NC 27706	
HQDA (DAMO-SSC)	1
HQDA (DAMA-ARZ, Dr. Verderame)	1
HQDA (DAMA-CSM-CM)	1
HQDA (DAMI-FIT)	1
WASH DC 20310	
US ARMY MATERIEL DEVELOPMENT AND READINESS COMMAND	
Commander	
US Army Materiel Development and Readiness Command	
Attn: DRCDE-DM	1
Attn: DRCLDC	1
Attn: DRCMT	1
Attn: DRCSF-S	1
Attn: DRCDL (Mr. N. Klein)	1
Attn: DRCBI (COL Gearin)	1
Attn: DRCDMD-ST (Mr. T. Shirata)	1
5001 Eisenhower Ave.	
Alexandria, VA 22333	
Commander	
US Army Foreign Science & Technology Center	
Attn: DRXST-MT-2	1
Attn: DRXST-CE (Mr. V. Rague)	1
220 Seventh St., NE	
Charlottesville, VA 22901	
Commander	
US Army Missile Command	
Redstone Scientific Information Center	
Attn: Chief, Documents	1
Attn: DRDMI-CGA (Dr. B. Fowler)	1
Attn: DRDMI-TE (Mr. H. Anderson)	1
Attn: DRDMI-KL (Dr. W. Wharton)	1
Redstone Arsenal, AL 35809	
US ARMY ARMAMENT RESEARCH AND DEVELOPMENT COMMAND	
Commander	
US Army Armament Research and Development Command	
Attn: DRDAR-TSS	5
Dover, NJ 07801	
US ARMY ARMAMENT MATERIEL READINESS COMMAND	
Commander	
US Army Armament Materiel Readiness Command	
Attn: DRSAR-ASN	1
Attn: DRSAR-PE	1
Rock Island, IL 61299	

PRECEDING PAGE NOT FILMED BLANK

DISTRIBUTION LIST FOR ARCSL-TR-79050 (Contd)

Names	Copies
Commander Harry Diamond Laboratories Attn: DRXDO-RDC (Mr. D. Giglio) 2800 Powder Mill Road Adelphi, MD 20783	1
Chief, Office of Missile Electronic Warfare US Army Electronic Warfare Laboratory Attn: DRSEL-WLM-SE (Mr. K. Larson) White Sands Missile Range, NM 88002	1
Project Manager for Smoke/Obscurants Attn: DRCP-SMK Aberdeen Proving Ground, MD 21005	2
Commander Atmospheric Sciences Laboratory	
Attn: DRSEL-BR-AS-P	1
Attn: DRSEL-BR-MS-A (Dr. R. Gomez)	1
Attn: DRSEL-BL-AS-DP (Mr. J. Lindberg)	1
Attn: DRSEL-BL-SY (Mr. F. Horning)	1
White Sands Missile Range, NM 88002	
Director US Army Materiel Systems Analysis Activity	
Attn: DRXSY-D (Dr. Fallin)	1
Attn: DRXSY-MP	1
Aberdeen Proving Ground, MD 21005	
Director Night Vision Laboratories	
Attn: DRSEL-NV-VI (Mr. R. Moulton)	1
Attn: DRSEL-NV-VI (Mr. R. Bergemann)	1
Fort Belvoir, VA 23651	
US Army Mobility Equipment Research and Development Center Attn: Code/DROME-RT (Mr. O. F. Kezer) Fort Belvoir, VA 22060	1
Commander US Army Electronics Command	
Attn: DRSEL-CT-LG (Dr. R. G. Rohde)	1
Attn: DRSEL-CT-1 (Dr. R. G. Buser)	1
Attn: DRSEL-WL-S (Mr. J. Charlton)	1
Fort Monmouth, NJ 07703	
Director US Army Ballistic Research Laboratories	
Attn: DRXBR-DL (Mr. T. Finnerty)	1
Attn: DRXBR-P (Mr. N. Gerri)	1
Attn: DRDAR-BLB (Mr. R. Reitz)	1
Attn: DRDAR-BLB (Mr. A. LaGrange)	1
Aberdeen Proving Ground, MD 21005	
CDR, APG	
Attn: STEAP-AD-R/RHA	1
Attn: STEAP-TL	1
Aberdeen Proving Ground, MD 21005	
Commander US Army Test & Evaluation Command Attn: DRSTE-FA Aberdeen Proving Ground, MD 21005	1
Commander Dugway Proving Ground	
Attn: STEDP-PO	1
Attn: Technical Library, Docu Sec	1
Attn: STEDP-MT-DA-E	1
Attn: STEDP-MT (Dr. L. Salamon)	1
Dugway, UT 84022	
US ARMY TRAINING & DOCTRINE COMMAND	
Commandant US Army Infantry School Combat Support & Maintenance Dept Attn: NBC Division Fort Benning, GA 31905	1
Commandant US Army Missile & Munitions Center & School	
Attn: ATSK-CD-MD	1
Attn: ATSK-DT-MU-EOD	1
Redstone Arsenal, AL 35809	
Commander US Army Logistics Center Attn: ATCL-MM Fort Lee, VA 23801	1
Commander HQ, USA TRADOC Attn: ATCD-TEC (Dr. M. Pastel) Fort Monroe, VA 23651	1
Commander US Army Ordnance & Chemical Center & School	
Attn: ATSL-CD-MS	1
Attn: ATSL-CD-MS (Dr. T. Welsh)	1
Aberdeen Proving Ground, MD 21005	
DEPARTMENT OF THE NAVY	
Commander Naval Surface Weapons Center Attn: Tech Lib & Info Svcs Br White Oak Laboratory Silver Spring, MD 20910	1
Commander Naval Intelligence Support Center 4301 Suitland Road Washington, DC 20390	1
Commander Naval Surface Weapons Center Dahlgren Laboratory Attn: DX-21 Dahlgren, VA 22448	1

DISTRIBUTION LIST FOR ARCSL-TR-79050 (Contd)

Names	Copies
Commander Naval Weapons Center	
Attn: Code 3311 (Dr. R. Bird)	1
Attn: Code 382 (Dr. P. St. Amand)	1
Attn: Code 3822 (Dr. Hindman)	1
China Lake, CA 93555	
Commanding Officer Naval Weapons Support Center	
Attn: Code 5041 (Mr. D. Johnson)	1
Attn: Code 5042 (Mr. C. Dinerman)	1
Crane, IN 47522	
Commander Naval Research Laboratory	
Attn: Code 5709 (Mr. W. E. Howell)	1
4555 Overlook Avenue, SW Washington, DC 20375	

Names	Copies
DEPARTMENT OF THE AIR FORCE	
HQ, Foreign Technology Division (AFSC) Attn: PDRR Wright-Patterson AFB, OH 45433	1
Commander Armament Development & Test Center Attn: DLOSL (Technical Library) Eglin AFB, FL 32542	1
Commander USEUCOM Attn: ECJ-O/LTC James H. Alley APO, NY 09128	1